PB88-171855

Exact Image Theory for the Problem of Dielectric/Magnetic Slab

Helsinki Univ. of Technology, Espoo (Finland)

Prepared for

National Aeronautics and Space Administration
Washington, DC

May 87

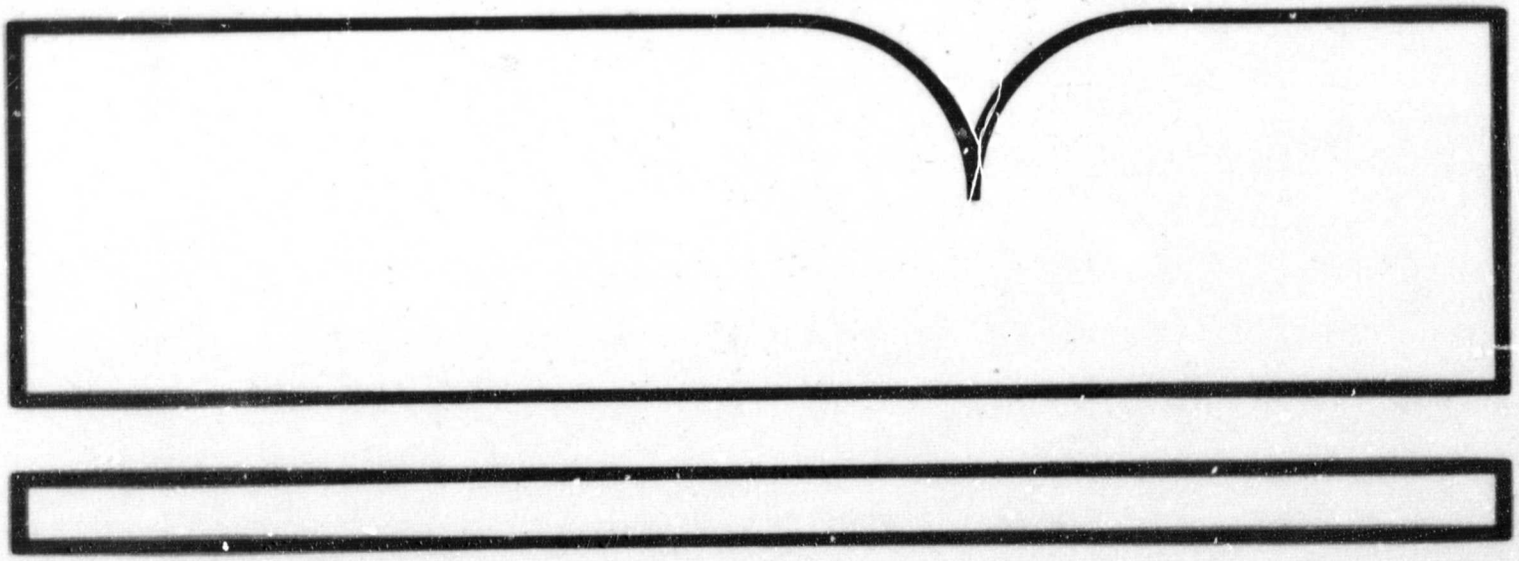

BIBLIOGRAPHIC INFORMATION

PB88-171855

Exact Image Theory for the Problem of Dielectric/Magnetic Slab,

May 87

by I. V. Lindell.

PERFORMER: Helsinki Univ. of Technology, Espoo (Finland). Electromagnetics Lab.
ISBN-951-754-241-0, REPT-16
Contracts N00014-83-K-0528, DAAG29-85-K-0079

SPONSOR: National Aeronautics and Space Administration, Washington, DC.

Sponsored in part by Grant NAG5-270. Sponsored by National Aeronautics and Space Administration, Washington, DC., Office of Naval Research, Arlington, VA., and Army Research Office, Research Triangle Park, NC.

Exact image method, recently introduced for the exact solution of electromagnetic field problems involving homogeneous half spaces and microstrip-like geometries, is developed here for the problem of homogeneous slab of dielectric and/or magnetic material in free space. Expressions for image sources, creating the exact reflected and transmitted fields, are given and their numerical evaluation is demonstrated. Nonradiating modes, guided by the slab and responsible for the loss of convergence of the omage functions, are considered and extracted. The theory allows, for example, an analysis of finite ground planes in microstrip antenna structures.

KEYWORDS: *Magnetic materials, *Dielectrics, *Foreign technology.

Available from the National Technical Information Service, SPRINGFIELD, VA. 22161

PRICE CODE: PC E03/MF A01

Exact Image Theory for the Problem of Dielectric/Magnetic Slab

Ismo V. Lindell

Helsinki University of Technology
Faculty of Electrical Engineering
Electromagnetics Laboratory

Otakaari 5 A, SF-02150 Espoo, Finland

Report 16

May 1987

EXACT IMAGE THEORY FOR THE PROBLEM OF DIELECTRIC/MAGNETIC SLAB

Ismo V. Lindell

Report 16, May 1987

ABSTRACT

Exact image method, recently introduced for the exact solution of electromagnetic field problems involving homogeneous half spaces and microstrip-like geometries, is developed here for the problem of homogeneous slab of dielectric and/or magnetic material in free space. Expressions for image sources, creating the exact reflected and transmitted fields, are given and their numerical evaluation is demonstrated. Nonradiating modes, guided by the slab and responsible for the loss of convergence of the omage functions, are considered and extracted. The theory allows, for example, an analysis of finite ground planes in microstrip antenna structures.

This work was funded by the Academy of Finland and, in part, by NASA grant NAG5-270, ONR contracts N00014-83-K-0528 and N00014-86-K-0533, and ARO contract DAAG-29-85-K-0079.

INTRODUCTION

Exact image theory, originally introduced for the Sommerfeld half-space problem [1], [2] was later generalized to the microstrip geometry [3], [4] consisting of a dielectric slab plus a perfectly conducting ground plane. To account for the more realizable case of finite ground plane, it is necessary to further extend the theory to the dielectric slab geometry, because the currents in the ground plane can then be solved through integral equation formulation. This problem was recently worked upon by Mosig [5] by using a numerical method to evaluate the ill-behaved Sommerfeld integrals. Because such integrals could be avoided in earlier applications of the exact image theory, the same principle suggests itself also for the present geometry.

The present paper is a continuation to the previous microstrip paper [4] with a minimal change in notation. The medium in the present case, however, is assumed to be more general, with both electric and magnetic susceptibility, and also the image giving the exact field transmitted through the slab will be developed. Because of this, the expressions have grown in extension and complexity in comparison to those of [4]. The complexity in image expressions is not, however, a major problem in the field calculation, because the image functions need only be calculated once for storage in the computer memory, after which their repetitive use in solving integral equations in the presence of the slab is possible with the present method.

BASIC THEORY

The solution of the dielectric slab problem can be obtained by decomposing the original source into symmetric and antisymmetric parts, which correspond to problems involving microstrip-type geometry. In fact, because of the symmetries of the corresponding fields, a plane of perfect conductor or magnetic conductor can be placed at the plane of symmetry in the middle of the slab and thus the problem is split up in two parts, one with the microstrip geometry and the other with the magnetic conductor microstrip geometry.

It is, however, preferable to make a fresh start for the slab geometry, because it is no more complicated than the study of magnetic conductor microstrip problem. Also, we are going to study the general dipole source above a slab with both electric and magnetic discontinuity and not just a transverse dipole at a dielectric interface as was done in [4]. However, the start with Fourier transforms similar to that in [1, part III], [4] will not be repeated here. The notation will be compatible with that in [4], with minor obvious changes.

The reflection dyadic for the electric field transverse to the z direction can be easily written from the partial wave reflection geometry, Fig. 1, from the knowledge that TE and TM polarizations are its eigenvectors:

$$\bar{\bar{R}} = R^{TE}\frac{\bar{K}\bar{K}\times\bar{u}\bar{u}}{K^2} + R^{TM}\frac{\bar{K}\bar{K}}{K^2} = (1-e^{-j\beta_1 4d})\bar{\bar{r}}\cdot(\bar{\bar{I}}_t - \bar{\bar{r}}^2 e^{-j\beta_1 4d})^{-1}, \qquad (1)$$

with $\bar{\bar{I}}_t = \bar{\bar{I}} - \bar{u}\bar{u}$, the two-dimensional unit dyadic and $\bar{\bar{r}}$ is the interface reflection dyadic. The inverse dyadic must be understood as a two-dimensional inverse [8]. We can further write

$$R^{TE,TM} = r^{TE,TM} + \sum_{n=1}^{\infty}\left((r^{TE,TM})^{2n+1} - (r^{TE,TM})^{2n-1}\right)e^{-j\beta_1 4nd}$$

$$= \frac{(1 - e^{-j\beta_1 4d}) r^{TE,TM}}{1 - (r^{TE,TM})^2 e^{-j\beta_1 4d}}, \tag{2}$$

$$\bar{\bar{r}} = r^{TE} \frac{\bar{K}\bar{K} \times \bar{u}\bar{u}}{K^2} + r^{TM} \frac{\bar{K}\bar{K}}{K^2}, \tag{3}$$

$$r^{TE} = \frac{\mu\beta - \beta_1}{\mu\beta + \beta_1}, \quad r^{TM} = -\frac{\epsilon\beta - \beta_1}{\epsilon\beta + \beta_1}. \tag{4}$$

Here, $\bar{K}$ is the two-dimensional Fourier variable on the plane transverse to the $\bar{u}$ vector and $\beta = \sqrt{k^2 - K^2}, \beta_1 = \sqrt{\mu\epsilon k^2 - K^2}$ are the propagation coefficients of the Fourier transformed wave in z coordinate (direction $\bar{u}$). Note that the thickness of the slab is denoted by $2d$ to be compatible with the microstrip substrate thickness d of [4].

Also, the field transmitted through the slab can be calculated from the knowledge of the total transmission dyadic, which is of the form

$$\bar{\bar{T}} = T^{TE} \frac{\bar{K}\bar{K} \times \bar{u}\bar{u}}{K^2} + T^{TM} \frac{\bar{K}\bar{K}}{K^2}, \tag{5}$$

$$T^{TE,TM} = \sum_{n=0}^{\infty} \left((r^{TE,TM})^{2n} - (r^{TE,TM})^{2n+2} \right) e^{-j\beta_1 (2n+1) 2d}. \tag{6}$$

From (2), (6) there results a relation between the reflection and transmission coefficients, and (5) can be given different dyadic forms:

$$\bar{\bar{T}} = (\bar{\bar{I}}_t - \bar{\bar{R}} \cdot \bar{\bar{r}}) e^{-j\beta_1 2d} = e^{-j\beta_1 2d} (\bar{\bar{I}}_t - \bar{\bar{r}}^2) \cdot \left(\bar{\bar{I}}_t - \bar{\bar{r}}^2 e^{-j\beta_1 4d} \right)^{-1} = \frac{1}{2} (\bar{\bar{R}}_m - \bar{\bar{R}}_e), \tag{7}$$

where $\bar{\bar{R}}_m$, $\bar{\bar{R}}_e$ are the reflection dyadics of the microstrip geometry with magnetic and electric conductor ground planes, respectively. As a check we see that for $\bar{\bar{r}}^2 = 0$, or $= \bar{\bar{I}}_t$, we have respectively from (7), $\bar{\bar{T}} = \bar{\bar{I}}_t e^{-j\beta_1 2d}$, or $= 0$, which correspond to the cases of perfectly transparent and perfectly reflecting slab.

The reflected and transmitted transverse electric fields can be written in the form given in [1, p.1028] for the general electric dipole $\bar{J}(\bar{r}) = \bar{v} I L \delta(\bar{r} - \bar{u}h)$ as follows:

$$\bar{e}(\bar{K}, z) = -(\bar{a} + j\beta\bar{b}) \cdot \bar{\bar{R}} \frac{e^{-j\beta(z+h)}}{2j\beta}, \quad for\ z > 0 \tag{8}$$

$$\bar{e}(\bar{K}, z) = -(\bar{a} + j\beta\bar{b}) \cdot \bar{\bar{T}} \frac{e^{j\beta(z-h+2d)}}{2j\beta}, \quad for\ z < -2d \tag{9}$$

with

$$\bar{a} = jk^{-1}\eta(k^2 \bar{\bar{I}}_t - \bar{K}\bar{K}) \cdot \bar{v} I L, \quad \bar{b} = k^{-1}\eta \bar{K} I L (\bar{u} \cdot \bar{v}). \tag{10}$$

To calculate the image for a transversal source, the reflection dyadic can be split up into two parts as was made in [4]:

$$\bar{\bar{R}} = R^{TE} \bar{\bar{I}}_t + R_0 \frac{\bar{K}\bar{K}}{k^2}, \tag{11}$$

where we have

$$R_0 = \frac{k^2}{K^2}(R^{TM} - R^{TE}) = \frac{(1 - e^{-j\beta_1 4d})(1 + r^{TE} r^{TM} e^{-j\beta_1 4d})}{(1 - (r^{TE})^2 e^{-j\beta_1 4d})(1 - (r^{TM})^2 e^{-j\beta_1 4d})} r_0, \tag{12}$$

with [1, p.1029]

$$r_0 = \frac{k^2}{K^2}(r^{TM} - r^{TE}) = \frac{1 - \mu^2}{\mu(\mu - \epsilon)}(r^{TE} - M) - \frac{1 - \epsilon^2}{\epsilon(\epsilon - \mu)}(r^{TM} + E), \tag{13}$$

$$E = \frac{\epsilon - 1}{\epsilon + 1}, \quad M = \frac{\mu - 1}{\mu + 1}. \tag{14}$$

To be able to construct image functions, the reflection coefficents are first expressed in terms of the reflection variable r, (which equals r^{TE} for $\mu = 1$ and $-r^{TM}$ for $\epsilon = 1$):

$$r = \frac{\beta - \beta_1}{\beta + \beta_1}. \tag{15}$$

Thus, we have

$$r^{TE} = \frac{M + r}{1 + Mr}, \tag{16}$$

$$r^{TM} = -\frac{E + r}{1 + Er}, \tag{17}$$

$$r_0 = \frac{4}{\mu - \epsilon}\left(\frac{1}{1 + Mr} - \frac{1}{1 + Er}\right). \tag{18}$$

The reflection coefficients R^{TE}, R^{TM} were given as power series of r^{TE}, r^{TM} in (2). For R_0 the following series can be written from (12):

$$R_0 = (1 - e^{-j\beta_1 4d}) r_0 \sum_{m=0}^{\infty} \sum_{n=0}^{\infty} K_{mn} (r^{TE})^m (r^{TM})^n e^{-j\beta_1 (m+n) 2d}, \tag{19}$$

where K_{mn} equals 1 when both m and n are even or odd, and = 0 otherwise, or explicitly, $K_{mn} = [1 + (-1)^{m+n}]/2$. Another form, less symmetric than (19), but better suited to successive computation of terms, is the following:

$$R_0 = r_0 \sum_{q=0}^{\infty} \sum_{i=0}^{2q} (r^{TE})^{2q-i} (r^{TM})^i \left(e^{-j\beta_1 q 4d} - e^{-j\beta_1 (q+1) 4d}\right). \tag{19a}$$

Whichever form of (19), (19a) is used, (16) and (17) can be substituted to obtain representations in terms of powers of the reflection variable r.

Like in the previous papers [1] - [4], the reflection coefficients will be presented as integral transforms of Laplace type to obtain image source functions. To this end, the following integral identity, invoked from [4], will be applied:

$$r^m e^{-j\beta_1 c} = \int_0^{\infty} [F_m(c, t) + \delta_{m0}\delta(t - c)]\, e^{-j\beta t} dt. \tag{20}$$

Here and henceforth, the delta function $\delta(x)$, also denoted $\delta_+(x)$ in [1], is defined to be zero for $x \leq 0$ so that $\int_0^\infty \delta(x)dx = 1$. $F_m(c,t)$ is the following function:

$$F_0(c,t) = \frac{B^2 c}{\tau} I_1(\tau) U(t-c), \tag{21}$$

$$F_m(c,t) = -\frac{B^2}{2\tau}\Big((t-c)I_{2m+1}(\tau) - (t+c)I_{2m-1}(\tau)\Big)\left(\frac{t-c}{t+c}\right)^m U(t-c) =$$

$$= -\frac{B}{2}\left[(B(t-c))^{2m+1}\frac{I_{2m+1}(\tau)}{\tau^{2m+1}} - (B(t-c))^{2m-1}\frac{I_{2m-1}(\tau)}{\tau^{2m-1}}\right] U(t-c), \quad m > 0, \tag{22}$$

with

$$B = k\sqrt{p^2 - 1}, \qquad \tau = B\sqrt{t^2 - c^2}. \tag{23}$$

$U(t)$ is the Heaviside unit step function making each function satisfy $F_m(c,t) = 0$ for $t < c$, and $I_n(\tau)$ denotes the modified Bessel function. For $c = 0$ (21), (22) reduce to

$$F_0(0,t) = 0, \quad F_m(0,t) = \frac{2m}{t} I_{2m}(Bt) U(t). \tag{24}$$

Further, we need the following expansions [4]

$$(r^{TM})^n = \sum_{k=0}^{\infty} C_k^n(E) r^k, \tag{25}$$

$$(r^{TE})^n = (-1)^n \sum_{k=0}^{\infty} C_k^n(M) r^k, \tag{26}$$

where the coefficient function is defined by

$$C_k^n(x) = \sum_{j=0}^{n|k} \frac{(-1)^j n(n+k-j-1)!}{(n-j)!j!(k-j)!}(-x)^{n+k-2j}, \quad n > 0, \tag{27}$$

$$C_k^0(x) = \delta_{0k}, \quad C_0^n(x) = (-x)^n,$$

$$C_k^1(x) = (-x)^{k+1} - (-x)^{k-1}, \quad C_1^n(x) = n[(-x)^{n+1} - (-x)^{n-1}].$$

Here, $n|k$ denotes the smaller of the numbers n and k. Values for the function can also be computed by reflection:

$$C_k^n(x) = \frac{n}{k} C_n^k(x), \quad k, n > 0, \tag{28}$$

and using the recursive formula

$$C_k^n(x) = -\frac{1}{x} C_k^{n-1}(x) - \frac{x^2 - 1}{x} \sum_{p=0}^{k} (-x)^{k-p} C_p^{n-1}(x). \tag{29}$$

(29) is more rapid than (27) if many values of $C_k^n(x)$ are to be calculated in computer memory for successive values of k and n with the same value of the argument x (constant ϵ or μ). The coefficient function $C_k^n(x)$ can also be defined through the expansion

$$tanh^n(\theta+\phi) = \sum_{k=0}^{\infty} C_k^n(tanh\theta)tanh^k\phi$$

VED REFLECTION IMAGE

Let us first construct the image due to the vertical dipole $\bar{J}(\bar{r}) = \bar{u}IL\delta(\bar{\rho})\delta(z-h)$, which lies at the distance $z = h$ from the slab. The transversal electric field in Fourier space is obtained from (8) when $\bar{v} = \bar{u}$:

$$\bar{e}(\bar{K},z) = -j\beta k^{-1}\eta\bar{K}ILR^{TM}\frac{e^{-j\beta(z+h)}}{2j\beta}. \tag{30}$$

If the reflection coefficient is written in the integral form

$$R^{TM} = \int_0^{\infty} f^{TM}(t)e^{-j\beta t}dt, \tag{31}$$

the field can be easily seen to arise from the equivalent image source [1]

$$I_i(t) = ILf^{TM}(t). \tag{32}$$

To find the image function $f^{TM}(t)$, the expansions (2), (17), (20) and (25) must be applied:

$$R^{TM} = \sum_{k=0}^{\infty} C_k^1(E)r^k + \sum_{m=1}^{\infty}\sum_{k=0}^{\infty}\left(C_k^{2m+1}(E) - C_k^{2m-1}(E)\right)r^k e^{-j\beta_1 4md}, \tag{33}$$

whence the following expression for the image function is obtained:

$$f^{TM}(t) = C_0^1(E)\delta(t) + \sum_{m=1}^{\infty}\left(C_0^{2m+1}(E) - C_0^{2m-1}(E)\right)\delta(t-4md)$$

$$+\sum_{k=1}^{\infty} C_k^1(E)F_k(0,t) + \sum_{m=1}^{\infty}\sum_{k=0}^{\infty}\left(C_k^{2m+1}(E) - C_k^{2m-1}(E)\right)F_k(4md,t). \tag{34}$$

Thus, the image function consists of a series of delta functions, corresponding to dipoles with interspaces $4d$, which is double the slab thickness, and a continuous source function. The function depends on both ϵ and μ through the variable B in the functions $F_k(x,t)$, and on ϵ through the functions $C_k^n(E)$. It is seen that the dipole images depend only on ϵ. Taking $\epsilon = 1$, or what is equivalent, $E = 0$, all the delta terms in (34) vanish because of the following limit of the function $C_k^n(x)$ as $x \to 0$:

$$C_k^n(0) = (-1)^n\delta_{kn}. \tag{35}$$

The vanishing of delta terms is also seen if (34) is written in the form

$$f^{TM}(t) = -\frac{\epsilon-1}{\epsilon+1}\delta(t) + \frac{4\epsilon}{\epsilon^2-1}\sum_{m=1}^{\infty}\left(\frac{\epsilon-1}{\epsilon+1}\right)^{2m}\delta(t-4md) \tag{34a}$$

$$-\frac{8\epsilon}{\epsilon^2-1}\sum_{k=1}^{\infty}k\left(-\frac{\epsilon-1}{\epsilon+1}\right)^{k}\frac{I_{2k}(Bt)}{t}U(t) + \sum_{m=1}^{\infty}\sum_{k=0}^{\infty}\left(C_k^{2m+1}(E) - C_k^{2m-1}(E)\right)F_k(4md,t).$$

To obtain this, (24) has been applied. For $\epsilon = 1$, all coefficients of the delta functions are seen to vanish. The remaining image function can be written as

$$f^{TM}(t) = -F_1(0,t) - \sum_{m=1}^{\infty}\left(F_{2m+1}(4md,t) - F_{2m-1}(4md,t)\right). \tag{36}$$

This expression can be compared with that given in [4] for the TE image with $\mu = 1$ in the microstrip problem.

VED TRANSMISSION IMAGE

The corresponding transmission image function can be obtained from the expressions (6), (20), (25) for T^{TM}. Thus, writing

$$T^{TM} = \int_0^{\infty} h^{TM}(t)e^{-j\beta t}dt = \sum_{n=0}^{\infty}\left((r^{TM})^{2n} - (r^{TM})^{2n+2}\right)e^{-j\beta_1(2n+1)2d}$$

$$= \sum_{n=0}^{\infty}\sum_{k=0}^{\infty}\left(C_k^{2n}(E) - C_k^{2n+2}(E)\right)r^k e^{-j\beta_1(2n+1)2d}, \tag{37}$$

we have

$$h^{TM}(t) = \sum_{n=0}^{\infty}\sum_{k=0}^{\infty}\left(C_k^{2n}(E) - C_k^{2n+2}(E)\right)\left[F_k((2n+1)2d,t) + \delta_{k0}\delta(t-(2n+1)2d)\right]$$

$$= \frac{4\epsilon}{(\epsilon+1)^2}\sum_{n=0}^{\infty}E^{2n}\delta(t-(2n+1)2d) + \sum_{n=0}^{\infty}\sum_{k=0}^{\infty}\left(C_k^{2n}(E) - C_k^{2n+2}(E)\right)F_k((2n+1)2d,t). \tag{38}$$

Similarly to the case for the reflection image function, if $\epsilon = 1$ the delta function (dipole) image terms vanish except for the first one, which corresponds to the original dipole source. The resulting function for $\epsilon = 1$ $(E = 0)$ is of the form

$$h^{TM}(t) = \delta(t-2d) + \sum_{n=0}^{\infty}\left[F_{2n}((2n+1)2d,t) - F_{2n+2}((2n+1)2d,t)\right]. \tag{39}$$

The transverse component of the TM electric field transmitted into the region $z < -2d$ can be written from (9)

$$e(\bar{K}, z) = j\beta k^{-1}\eta \bar{K} I L T^{TM} \frac{e^{j\beta(z-h)}}{2j\beta}. \tag{40}$$

When T^{TM} is expressed as in (37), (40) can be interpreted as the field arising from the image current

$$I_i(t) = IL h^{TM}(t), \tag{41}$$

where $h^{TM}(t)$ is of the form (38). Obviously, the transmission image has no counterpart in the microstrip problem.

HED REFLECTION IMAGE

The image current due to a horizontal (transverse) electric dipole $\bar{J}(\bar{r}) = \bar{v} I L \delta(\bar{\rho})\delta(z - h)$ can be divided into a horizontal and a vertical part [1], [4]. The horizontal part is obtained from the function $f^{TE}(t)$ defined through

$$R^{TE} = \int_0^\infty f^{TE}(t) e^{-j\beta t} dt. \tag{42}$$

Again, the reflection coefficient will be written as a power series of r:

$$R^{TE} = -\sum_{k=0}^{\infty} C_k^1(M) r^k - \sum_{m=1}^{\infty}\sum_{k=0}^{\infty} \left(C_k^{2m+1}(M) - C_k^{2m-1}(M)\right) r^k e^{-j\beta 4md}. \tag{43}$$

This leads to the following expression for the image function

$$f^{TE}(t) = -C_0^1(M)\delta(t) - \sum_{m=1}^{\infty} \left(C_0^{2m+1}(M) - C_0^{2m-1}(M)\right) \delta(t - 4md)$$

$$- \sum_{k=1}^{\infty} C_k^1(M) F_k(0,t) - \sum_{m=1}^{\infty}\sum_{k=0}^{\infty} \left(C_k^{2m+1}(M) - C_k^{2m-1}(M)\right) F_k(4md, t), \tag{44}$$

or, what is equivalent,

$$f^{TE}(t) = \frac{\mu - 1}{\mu + 1}\delta(t) - \frac{4\mu}{\mu^2 - 1} \sum_{m=1}^{\infty} \left(\frac{\mu - 1}{\mu + 1}\right)^{2m} \delta(t - 4md) \tag{44a}$$

$$+ \frac{8\mu}{\mu^2 - 1} \sum_{k=1}^{\infty} k \left(-\frac{\mu - 1}{\mu + 1}\right)^k \frac{I_{2k}(Bt)}{t} U(t) - \sum_{m=1}^{\infty}\sum_{k=0}^{\infty} \left(C_k^{2m+1}(M) - C_k^{2m-1}(M)\right) F_k(4md, t).$$

This is very similar to the function $f^{TM}(t)$ given above in (34). In fact, changing ϵ and μ, and the sign of the function $f^{TE}(t)$, the function $f^{TM}(t)$ is obtained, and vice versa. Thus, the same procedure of calculation can be used for both functions, which simplifies the use of the method. For $\mu = 1$ with (35), the expression (44) reduces to

$$f^{TE}(t) = F_1(0,t) + \sum_{m=1}^{\infty} [F_{2m+1}(4md,t) - F_{2m-1}(4md,t)], \tag{45}$$

which is in concord with that given in [4] for the microstrip geometry. In fact, a comparison shows us that (45) contains every second term of the microstrip image function, namely those with odd indices in the functions $F_k(c,t)$. For a microstrip with magnetic conductor ground plane, the sign of every second term (the even-indexed function terms) in the image function series is opposite to that of the normal microstrip. Thus, (45) is the average of the corresponding functions of the two microstrip problems. The microstrip image delta term due to the ground plane is absent in the slab geometry, because it is cancelled by the magnetic conductor term.

For the vertical part of the image current, a more complicated function $f_0(t)$ is needed:

$$R_0 = \int_0^{\infty} f_0(t) e^{-j\beta t} dt. \tag{46}$$

Applying (20) in (19) with (25), (26) inserted and defining

$$D_k^n(x) = xC_k^n(x) + C_k^{n+1}(x), \quad D_0^n(x) = 0, \tag{47}$$

the following expression for the reflection coefficient R_0 is obtained:

$$R_0 = \sum_{m=0}^{\infty}\sum_{n=0}^{\infty}\sum_{k=0}^{\infty}\sum_{l=0}^{\infty}(-1)^m K_{mn}\left(\frac{\mu^2-1}{\mu(\mu-\epsilon)}D_k^m(M)C_l^n(E) + \frac{\epsilon^2-1}{\epsilon(\epsilon-\mu)}C_k^m(M)D_l^n(E)\right)$$

$$\times r^{k+l}\left(e^{-j\beta_1(m+n)2d} - e^{-j\beta_1(m+n+2)2d}\right). \tag{48}$$

The symmetric double sums can be calculated more practically in the following way:

$$R_0 = \sum_{q=0}^{\infty}\left(e^{-j\beta_1 q4d} - e^{-j\beta_1(q+1)4d}\right)\sum_{s=0}^{\infty} r^s$$

$$\times \sum_{i=0}^{2q}\sum_{j=0}^{s}(-1)^i\left(\frac{\mu^2-1}{\mu(\mu-\epsilon)}D_{s-j}^{2q-i}(M)C_j^i(E) + \frac{\epsilon^2-1}{\epsilon(\epsilon-\mu)}C_{s-j}^{2q-i}(M)D_j^i(E)\right). \tag{48a}$$

Thus, the partial image function $f_0(t)$ can be written in the form

$$f_0(t) = \sum_{m=0}^{\infty}\sum_{n=0}^{\infty}\sum_{k=0}^{\infty}\sum_{l=0}^{\infty}(-1)^m K_{mn}\left(\frac{\mu^2-1}{\mu(\mu-\epsilon)}D_k^m(M)C_l^n(E) + \frac{\epsilon^2-1}{\epsilon(\epsilon-\mu)}C_k^m(M)D_l^n(E)\right)$$

$$\times [F_{k+l}((m+n)2d,t) - F_{k+l}((m+n+2)2d,t)], \tag{49}$$

or, corresponding to (48a), in the form

$$f_0(t) = \sum_{q=0}^{\infty}\sum_{s=0}^{\infty}[F_s(q4d,t) - F_s((q+1)4d,t)]$$

$$\cdot \sum_{i=0}^{2q}\sum_{j=0}^{s}\left(\frac{\mu^2-1}{\mu(\mu-\epsilon)}D_{s-j}^{2q-i}(M)C_j^i(E) + \frac{\epsilon^2-1}{\epsilon(\epsilon-\mu)}C_{s-j}^{2q-i}(M)D_j^i(E)\right). \qquad (49a)$$

The complicated appearance of the function $f_0(t)$ is counterbalanced by the fact that the functions $F_s(c,t)$ are zero for $t < c$, whence only a few terms must be actually calculated for low t values and, in many cases, the calculation can be stopped before the number of terms grows very large.

For the special case $\mu = 1$, or $M = 0$ the above function is simplified to

$$f_0(t) = \frac{\epsilon+1}{\epsilon}\sum_{m=0}^{\infty}\sum_{n=0}^{\infty}\sum_{l=0}^{\infty}K_{mn}D_l^n(E)[F_{m+l}((m+n)2d,t) - F_{m+l}((m+n+2)2d,t)]$$

$$= \frac{\epsilon+1}{\epsilon}\sum_{q=0}^{\infty}\sum_{s=0}^{\infty}[F_s(q4d,t) - F_s((q+1)4d,t)]\sum_{i=0}^{2q}D_{s+i-2q}^i(E). \qquad (50)$$

In (50), only terms with $s + i - 2q > 0$ contribute. This expression is in accord with the corresponding result (function $g(t)$) for the microstrip geometry given in [4].

The HED image current expression can be obtained from the combination of the horizontal and vertical partial image current functions $f^{TE}(t)$, $f_o(t)$, from a comparison of the resulting transverse electric field,

$$\bar{e}(\bar{K},z) = -jk\eta(\bar{\bar{I}}_t - k^{-2}\bar{K}\bar{K})\cdot R_0\frac{\bar{K}\bar{K}}{k^2}\cdot\bar{v}IL\frac{e^{+j\beta(z+h)}}{2j\beta}, \qquad (51)$$

with the corresponding free-space expression. This was done in [1, p.1029] for the Sommerfeld problem and in [4] for the microstrip problem and the resulting expressions for the image current source are essentially the same as here, with a difference in the choice of integration variable in [1] and notations for the image functions. Thus, we can write for the image of nay transverse source satisfying $\bar{u}\cdot\bar{J}(\bar{r}) = 0$,

$$\bar{J}_i(\bar{r},t) = f^{TE}(t)\bar{J}_c(\bar{r}) - \bar{u}k^{-2}f_0'(t)\nabla\cdot\bar{J}_c(\bar{r}), \qquad (52)$$

with

$$\bar{J}_c(\bar{r})' = \bar{\bar{C}}\cdot\bar{J}(\bar{\bar{C}}\cdot\bar{r}),\quad \bar{\bar{C}} = \bar{\bar{I}}_t - 2\bar{u}\bar{u}. \qquad (53)$$

It is seen that the effective function in the vertical current component is not $f_0(t)$, but its derivative $f_0'(t)$, which is in accord with the results of [1], [4].

HED TRANSMISSION IMAGE

The expressions for the transmission image for the transverse, or horizontal, source can be obtained much in the same way as above by seeking the horizontal and vertical partial images separately. The transmission dyadic is of the form

$$\bar{\bar{T}} = T^{TE}\bar{\bar{I}}_t + T_0\frac{\bar{K}\bar{K}}{k^2}, \tag{54}$$

Expressing the first transmission coefficient as

$$T^{TE} = \int_0^\infty h^{TE}(t)e^{-j\beta t}dt = \sum_{n=0}^{\infty}\left((r^{TE})^m - (r^{TE})^{2n+2}\right)e^{-j\beta_1(2n+1)2d}$$

$$= \sum_{n=0}^{\infty}\sum_{k=0}^{\infty}\left(C_k^{2n}(M) - C_k^{2n+2}(M)\right)r^k e^{-j\beta_1(2n+1)2d}, \tag{55}$$

we can write for the horizontal partial transmission image function,

$$h^{TE}(t) = \frac{4\mu}{(\mu+1)^2}\sum_{n=0}^{\infty}M^{2n}\delta(t-(2n+1)2d)$$

$$+\sum_{n=0}^{\infty}\sum_{k=0}^{\infty}\left(C_k^{2n}(M) - C_k^{2n+2}(M)\right)F_k((2n+1)2d,t). \tag{56}$$

This is the same function as $h^{TM}(t)$ if the change $\epsilon \leftrightarrow \mu$ is made, as is seen from (38). For $\mu = 1$ the form of the expression (39) is seen to result.

The vertical part of the HED transmission image is obtained from the transmission coefficient T_0:

$$T_0 = \int_0^\infty h_0(t)e^{-j\beta t}dt$$

$$= \frac{K^2}{k^2}\left(e^{-j\beta_1 2d} - e^{j\beta_1 6d}\right)\frac{(r^{TE})^2 - (r^{TM})^2}{(1-(r^{TE})^2e^{-j\beta_1 4d})(1-(r^{TM})^2\epsilon^{-j\beta_1 4d})}$$

$$= -r_0\sum_{n=0}^{\infty}\sum_{m=0}^{\infty}\left((r^{TM})^{2n}(r^{TE})^{2m+1} + (r^{TM})^{2n+1}(r^{TE})^{2m}\right)$$

$$\times\left(\epsilon^{-j\beta_1(2n+2m+1)2d} - e^{-j\beta_1(2n+2m+3)2d}\right). \tag{57}$$

Hence, the image function can be written in the following two forms

$$h_0(t) = -\sum_{n=0}^{\infty}\sum_{m=0}^{\infty}\sum_{k=0}^{\infty}\sum_{l=0}^{\infty}\Big[\frac{\mu^2-1}{\mu(\mu-\epsilon)}\left(D_k^{2m+1}(M)C_l^{2n}(E) - D_k^{2m}(M)C_l^{2n+1}(E)\right)$$

$$-\frac{\epsilon^2-1}{\epsilon(\epsilon-\mu)}\left(C_k^{2m+1}(M)D_l^{2n}(E) + C_k^{2m}(M)D_l^{2n+1}(E)\right)\Big].$$

$$\times[F_{k+l}((2m+2n+1)2d,t) - F_{k+l}((2m+2n+3)2d,t)], \tag{58}$$

$$h_0(t) = -\sum_{q=0}^{\infty}\sum_{s=0}^{\infty}[F_s((2q+1)2d,t) - F_s((2q+3)2d,t)]$$

$$\times \sum_{i=0}^{q}\sum_{j=0}^{s}\left[\frac{\mu^2-1}{\mu(\mu-\epsilon)}\left(D_{s-j}^{2(q-i)+1}(M)C_j^{2i}(E) - D_{s-j}^{2(q-i)}(M)C_j^{2i+1}(E)\right)\right.$$

$$\left.\frac{\epsilon^2-1}{\epsilon(\epsilon-\mu)}\left(C_{s-j}^{2(q-i)+1}(M)D_j^{2i}(E) + C_{s-j}^{2(q-i)}(M)D_j^{2i+1}(E)\right)\right]. \tag{58a}$$

The result has a bit more complicated appearance than the corresponding reflection image function $f_0(t)$ in (49), (49a). The difference arises from the difference in the partial wave structure, Fig.1. For the special case $\mu = 1$, (58a) reduces to

$$h_0(t) = \frac{\epsilon+1}{\epsilon}\sum_{q=0}^{\infty}\sum_{s=0}^{\infty}[F_s((2q+1)2d,t) - F_s((2q+3)2d,t)]\sum_{i=0}^{q}[D_s^{2i+1}(E) - D_s^{2i}(E)]. \tag{59}$$

GENERAL IMAGES

To obtain the reflection and transmission images of the general dipole, previous results can be combined. In short, for the general three-dimensional source function $\bar{J}(\bar{r})$ the reflection image is

$$\bar{J}_i(\bar{r},t) = \left(f^{TM}(t)\bar{u}\bar{u} + f^{TE}(t)\bar{\bar{I}}_t\right)\cdot\bar{J}_c(\bar{r}) - \bar{u}k^{-2}f_0'(t)\nabla_t\cdot\bar{J}_c(\bar{r}). \tag{60}$$

The reflection field can be obtained everywhere in the half space $z > 0$ through an integration of the free-space Green dyadic multiplied by the image:

$$\bar{E}(\bar{r}) = -jk\eta\int_0^{\infty}\int_V \bar{\bar{G}}(\bar{r}-\bar{r}'+\bar{u}t)\cdot\bar{J}_i(\bar{r}',t)dtdV'. \tag{61}$$

If the original source is a dipole or a planar current source of the form $\bar{J}(\bar{r}) = \bar{J}_s(\bar{\rho})\delta(z-h)$, the integration variable t can be disposed of, because in the field integral (61) any function of the form $G(\bar{r}-\bar{r}'+\bar{u}t)\phi(t)\delta(z'+h)$ can be replaced by the function $-G(\bar{r}-\bar{r}')\phi(-(z'+h))$, leaving out the t integration and taking the z' integration from $-h$ to $-\infty$. The image of the dipole consists of a set of dipoles and partially overlapping line sources along the negative real z axis, which start at the points $-(h+m4d)$, $m = 0,1,2,\ldots$.

For the general transmission image we have, correspondingly,

$$\bar{J}_i(\bar{r},t) = \left(h^{TM}(t)\bar{u}\bar{u} + h^{TE}\bar{\bar{I}}_t\right)\cdot\bar{J}(\bar{r}) - \bar{u}k^{-2}h_0'(t)\nabla_t\cdot\bar{J}(\bar{r}), \tag{62}$$

which produces the field in the half space $z < -2d$. The field can be obtained from the free-space integral

$$\bar{E}(\bar{r}) = -jk\eta \int_0^\infty \int_V \bar{\bar{G}}(\bar{r} - \bar{r}' - \bar{u}(t-2d)) \cdot \bar{J}_i(\bar{r}', t) dt dV'. \tag{63}$$

Again, for a dipole source, the image current function can be written without the t variable, because of the special $\delta(z' - h)$ dependence of the original current source. Hence, to calculate the field, instead of both t and z' integrations we need only make the z' integration taking $\phi(z' + 2d - h)$ instead of $\phi(t)$ and integrating z' from $h - 2d$ to $+\infty$. From the transmission image functions we can see that the final image consists of dipoles and partially overlapping line sources along the positive z axis, each starting at the points $h + (2m+1)2d$. Thus, the transmission image current starts at the height $h + 2d - 2d = h$, or from the original source point.

The images corresponding to magnetic sources can be obtained easily from the duality transform $I \rightarrow I_m, \epsilon \leftrightarrow \mu$. Note that ϵ and μ are relative quantities so that minus signs do not occur in this simple duality transform.

ASYMPTOTIC TESTS

To gain confidence in the above expressions, some of which have rather complicated appearance, it is necessary to perform asymptotic tests to see that correct limit cases are obtained. In fact, we should check that the image solution corresponds to

(A) for $\epsilon = 1$ and $\mu = 1$, the free-space problem
(B) for $\epsilon \rightarrow \infty$, the perfect conductor plane problem
(C) for $\mu \rightarrow \infty$, the perfect magnetic conductor plane problem
(D) for $d \rightarrow 0$, the free-space problem
(E) for $d \rightarrow \infty$, the Sommerfeld half-space problem.

The case (A) is easily seen to be satisfied, because $B = \sqrt{\mu\epsilon - 1} = 0$, whence the arguments of all Bessel functions in the definitions (21), (22) are zero, making the F_m functions vanish. Thus, from (36), (39), (45), (50), (56) and (58) we see that all the other images vanish except the delta function $\delta(t-2d)$ in the transmission image expressions, which corresponds to the original current as a transmission source and there is no reflection sources.

The cases (B) and (C) are more complicated. In case (B), $E = 1$ and from (27) we can derive the limit function needed here,

$$C_k^n(1) = (-1)^n \delta_{k0}. \tag{64}$$

Considering the VED source and inserting (64) in (34), it is seen that the sum expressions all vanish, because $F_0(0,t) = 0$ and the terms in brackets cancel. Thus, only the first delta term survives giving $f^{TM}(t) = -\delta(t)$, which together with the mirror operation, c in (59), leaves us with the positive image of the vertical dipole. This corresponds to the mirror image due to a conducting plane. Also, it is readily seen from (38) that the transmission image of a VED vanishes. For the HED, the outcome is not so simply seen, because the image functions do not explicitly depend on ϵ. The functions $F_m(c,t)$, however, depend on the parameter $B = \sqrt{\mu\epsilon - 1}$, which becomes large. Considering the image function expressions, we see that they can be written in the form $Bf(Bt)$, and denoting $x = Bt$, the field integral is of the form

$$\int_0^\infty G(t) B f(Bt) dt = \int_0^\infty G(\frac{x}{B}) f(x) dx \approx G(0) \int_0^\infty f(x) dx, \tag{65}$$

as $B \to \infty$. This means that the image can be replaced by a point source at $t = 0$, or $z = -h$. What the point source is, is seen after the integral is developed. It is not difficult to evaluate these integrals if the identity (20) is invoked. In fact, writing for $\beta = 0, \beta_1 = B$, we have

$$\int_0^\infty (F_m(c,t) + \delta_{m0}\delta(t-c))\,dt = (-1)^m e^{-jBc}, \tag{66}$$

and taking a vanishingly small negative phase angle for B, the right-hand side vanishes, whence the integral of $F_m(c,t)$ for $m > 0$ is seen to vanish and for $m = 0$ give the value -1. With this, checking all the components, we are able to show that for $\epsilon \to \infty$, the image current source can be replaced by

$$\bar{J}_i(\bar{r},t) \Rightarrow \delta(t)\int_0^\infty \bar{J}_i(\bar{r},t)dt = -\delta(t)\bar{J}_c(\bar{r}). \tag{67}$$

This is the mirror image due to the perfectly conducting plane at $z = 0$. In the same manner, the transmission image can be seen to vanish in this limit. Case (C) follows from (B) through the duality transformation.

In case (D), the functions $F_k(n2d,t)$ can be replaced by $F_k(0,t)$, whence in all image functions in the summations over the index n most of the terms are cancelled. This makes the reflection image functions $f^{TE}(t)$, $f^{TM}(t)$, $f_0(t)$ vanish together with the transmission image function $h_0(t)$, leaving only $h^{TE}(t) = h^{TM}(t) = \delta(t-2d)$, which corresponds to the primary source of the free-space problem.

Finally, in case (E), we should end up in the image of the Sommerfeld problem given in [1]. To conform with the notation in [1], a change of the variable from t to $p = jBt$ must be made. Then, writing from (24), we have

$$F_m(0,t) = \frac{2m}{t}I_{2m}(Bt)U(t) = jB(-1)^m\frac{2m}{p}J_{2m}(p)U(p), \tag{68}$$

which gives us the following relation of the present notation and the function $f_\alpha(p)$ of [1]:

$$\sum_{k=0}^{\infty} C_k^1(E)F_k(0,t) = -jBf_\epsilon(p). \tag{69}$$

In fact, the Sommerfeld image functions can be seen to result for the reflection image in the first interval from $t = 0$ to $t = -4d$ for any value of d. For $d \to \infty$, obviously other images are pushed to infinity and have no effect and the whole problem is reduced to the Sommerfeld problem. Concentrating on the interval $t = 0 \ldots -4d$, functions of the type $\delta(t-md)$ and $F_k(md,t)$ with $m > 0$ can be discarded, since they are zero up to $t = md$ and only terms with $\delta(t)$ and $F_k(0,t)$ survive. Thus, we can write in this interval from (34), (69):

$$f^{TM}(t) = -jB\left(\frac{\epsilon-1}{\epsilon+1}\delta(p) + f_\epsilon(p)\right), \tag{70}$$

$$f^{TE}(t) = jB\left(\frac{\mu-1}{\mu+1}\delta(p) + f_\mu(p)\right), \tag{71}$$

$$f_o(t) = -jB\left(\frac{\mu^2-1}{\mu(\mu-\epsilon)}f_\mu(p) + \frac{\epsilon^2-1}{\epsilon(\epsilon-\mu)}f_\epsilon(p)\right) = -jBg(p). \tag{72}$$

Because $f_0'(t) = (jB)^2 g'(p)$, we have from the general image of (60)

$$\tilde{J}_i(\bar{r},t) = jB\bar{J}_i(\bar{r},p), \quad or \quad \tilde{J}_i(\bar{r},t)dt = \bar{J}_i(\bar{r},p)dp, \tag{73}$$

where the left-hand sides refer to the present theory and the right-hand sides to the corresponding function of the Sommerfeld problem as given in [1, p.1030]. Thus, the image function in the slab problem in the interval $t = 0... - 4d$ is only dependent on the first interface, corresponding to the first reflected partial ray in Fig. 1.

As an encore, we briefly show how the delta function terms in image functions can be obtained directly from the reflection coefficient expressions as a limit when $\beta \to \infty$. This corresponds to the simpler analysis of the delta function part of the VED image given in [1, Part II]. Studying (2) for this limit, whence $\beta_1 \to \beta$, we see that because $r^{TM} \to -E$, from the limit expression of R^{TM}, eqn. (2), denoted by R_δ^{TM}, we have the equation

$$(1 - E^2 e^{-4j\beta d})R_\delta^{TM} = -E(1 - e^{-4j\beta d}). \tag{74}$$

This can be readily Laplace transformed to a difference equation for the corresponding image function $f_\delta^{TM}(t)$:

$$f_\delta^{TM}(t)U(t) - E^2 f_\delta^{TM}(t - 4d)U(t - 4d) = -E\delta(t) + E\delta(t - 4d). \tag{75}$$

The solution of this is obtained quite straightforwardly:

$$f_\delta^{TM}(t) = -E\delta(t) + \sum_{n=1}^{\infty}\left((-E)^{2n+1} - (-E)^{2n-1}\right)\delta(t - 4nd), \tag{76}$$

which is exactly the delta-function part of (34).

GUIDED MODES

It was seen in the analysis of the microstrip geometry [3], [4] that some of the image functions would not converge along the real z axis and the reason was found to be in the nonradiating guided modes. After extracting the exponentially diverging image terms corresponding to these modes, the remaining image was convergent. The number of nonradiating modes was dependent on the frequency and medium parameters, but there was at least one such mode (TM mode) for the microstrip. The same applies for the slab except that there exist at least two such modes (TE and TM) in the slab. After extraction of these modes, the image functions are convergent.

The modes can be classified in four groups in terms of TE/TM polarization and properties of symmetry/antisymmetry of the transverse modal electric field. Antisymmetric modes correspond to those existing in the microstrip structure, whereas the symmetric ones exist in the microstrip with magnetic conducting ground plane.

The modes are obtained from the poles of the reflection coefficients, all of which appear in the expression (12). The poles $\beta = \beta_p$, $\beta_1 = \beta_{1p}$ are obtained as roots of the four equations

$$r^{TE,TM}(\beta,\beta_1)e^{-j\beta_1 2d} = \pm 1. \tag{77}$$

These equations can also be written as

$$r^{TM}e^{-j\beta_1 2d} = 1, \quad or \quad \frac{\beta_1}{\omega\epsilon\epsilon_0} jtan(\beta_1 d) = -\frac{\beta}{\omega\epsilon_0}, \tag{77a}$$

$$r^{TM}e^{-j\beta_1 2d} = -1, \quad or \quad \frac{\beta_1}{\omega\epsilon\epsilon_0}[-jcot(\beta_1 d)] = -\frac{\beta}{\omega\epsilon_0}, \tag{77b}$$

$$r^{TE}e^{-j\beta_1 2d} = 1, \quad or \quad \frac{\omega\mu\mu_0}{\beta_1} jtan(\beta_1 d) = -\frac{\omega\mu_0}{\beta}, \tag{77c}$$

$$r^{TE}e^{-j\beta_1 2d} = -1, \quad or \quad \frac{\omega\mu\mu_0}{\beta_1}[-jcot(\beta_1 d)] = -\frac{\omega\mu_0}{\beta}. \tag{77d}$$

The right-hand equations of (77a), (77c) correspond to transverse impedance interpretation of the problem with a conducting plane in the middle of the slab and those of (77b), (77d) the same with a magnetically conducting plane. Thus, the problem is reduced to finding the modes in microstrip and magnetic microstrip structures. Each root of (77a) - (77d) corresponds to a guided mode in the slab. For sufficiently low values of $Bd = \sqrt{\mu\epsilon - 1}kd$, only one TE and one TM mode have field dependencies that are decaying in the z direction (imaginary β) and can be considered as nonradiating waveguide modes in the slab. These modes correspond to lowest solutions of (77a) and (77d), which can be obtained with the method described in [4]. Defining $q = \beta_{1p}d$, we have for both the TM and TE wave

$$qtanq = \gamma\sqrt{(Bd)^2 - q^2}, \tag{78}$$

where $\gamma = \epsilon$ for the TM wave and $\gamma = \mu$ for the TE wave. The lowest solution for small values of Bd can easily be obtained, starting from $q_0 = Bd$ in the iteration formula [4]

$$q_{n+1} = Bd\sqrt{1 - (q_n tanq_n/\gamma Bd)^2}, \tag{79}$$

after which β_p is obtained from (77a)-(77d). For real Bd, the graphical solution of Fig.2 can also be applied. In Fig.3, values of $\alpha_p d = j\beta_p d$ for different Bd and ϵ or μ values are given, corresponding to the respective cases of TM and TE waveguide modes.

Because the guided mode is nonradiating, the corresponding pole satisfies $Im[\beta_p] < 0$, which corresponds to an exponentially diverging reflection image current. This must be extracted from the image function to obtain a converging source. For this purpose, residue of the reflection coefficient at the pole must be calculated. We can write the TE and TM reflection coefficients in the same form

$$R = R' + \frac{A_p}{\beta - \beta_p}, \tag{80}$$

with $\beta_p = -j\alpha_p$, the basic pole and A_p, the corresponding residue

$$A_p = \pm\frac{\gamma\beta_p\beta_{1p}^2}{\gamma B^2 - j\beta_p d(\gamma^2\beta_p^2 - \beta_{1p}^2)}, \quad \beta_{1p} = \sqrt{\beta_p^2 + B^2}. \tag{81}$$

For the TE wave, the uppersign and $\gamma = \mu$ must be taken, while for the TM wave, lower sign and $\gamma = \epsilon$ applies.

In the limit $Bd \to 0$, the lowest root is $q = \beta_{1p}d \approx Bd$, whence $\beta_p d = -j\alpha_p d = (-j\beta_{1p}d/\gamma)tan\beta_{1p}d \approx -j(Bd)^2/\gamma$. In this case, the residue (81) reduces to $A_p \approx \pm\beta_p \approx \mp jB^2 d/\gamma$. The nondiverging part of the image function is $f(t) - jA_p e^{j\beta_p t} \approx f(t) \mp (B^2 d/\gamma)exp(B^2 dt/\gamma)$.

The function $jA_p e^{j\beta_p t}$, subtracted from the image function, diverges for real t and must be moved into another position on the complex t plane, as described in [3] and [4].

CALCULATION OF IMAGE FUNCTIONS

Finally, let us study numerical properties of the different image functions. The function $F_n(c,t)$ was defined in (21), (22) in terms of modified Bessel functions. For small argument values, the following power series, based on Taylor expansion of Bessel functions, can be applied [4]:

$$F_0(c,t) = \frac{B^2 c}{2} \sum_{k=0}^{\infty} \frac{x^k y^k}{k!(k+1)!} U(t-c),$$

$$F_n(c,t) = -\frac{B}{2} \sum_{k=0}^{\infty} \frac{x^k}{k!} \left(\frac{y^{2n+k+1}}{(2n+k+1)!} - \frac{y^{2n+k-1}}{(2n+k-1)!} \right) U(t-c), \quad n > 0 \qquad (82)$$

with

$$x = \frac{B(t+c)}{2}, \quad y = \frac{B(t-c)}{2}.$$

Another method suitable for microcomputer use is to apply polynomial approximations for the modified Bessel functions $I_0(x)$, $I_1(x)$ and to compute functions with other indices from the recursive formula [7], after which (21), (22) can be applied.

Examples of the normalized function $\frac{2}{B}F_n(c,t)$ are depicted in Fig.4 for different values of n and Bc. Because the modified Bessel functions $I_n(x)$ diverge asymptotically as $e^x/\sqrt{2\pi x}$ for all n, the F_n functions diverge for $t \to \infty$ as

$$F_n(c,t) \to \frac{Bc}{\sqrt{2\pi B t^3}} e^{Bt}. \qquad (83)$$

It was seen in [4] for the microstrip geometry that, in spite of the divergence of the individual F_n terms in the image function series expression, the whole function may be well convergent within the limit of computer accuracy.

The functions $F_m(c,t)$ can be grouped for better convergence. For example, denoting $\tau_m = B\sqrt{t^2 - (4md)^2}$, the special TM function of (36) can be written as

$$\begin{aligned}
\frac{2}{B} f^{TM}(t) = &- \left(I_1(Bt)U(t) - B(t-4d)\frac{I_1(\tau_1)}{\tau_1} U(\tau_1) \right) \\
&+ \left(I_3(Bt)U(t) - (B(t-4d))^3 \frac{I_3(\tau_1)}{\tau_1^3} U(\tau_1) \right) \\
&- \left((B(t-4d))^5 \frac{I_5(\tau_1)}{\tau_1^5} U(\tau_1) - (B(t-8d))^5 \frac{I_5(\tau_2)}{\tau_2^5} U(\tau_2) \right) \\
&+ \left((B(t-4d))^7 \frac{I_7(\tau_1)}{\tau_1^7} U(\tau_1) - (B(t-8d))^7 \frac{I_7(\tau_2)}{\tau_2^7} U(\tau_2) \right) - \ldots . \qquad (84)
\end{aligned}$$

For values of Bd satisfying $Bd < \pi/2$ there only exists one nonradiating guided TM mode, whose parameters can be obtained from (78). For small values of Bd, we can write the two-term approximation of the function (84) with the pole term removed in the following simple form:

$$\frac{2}{B}\left(f^{TM}(t) - jA_p e^{j\beta_p t}\right) \approx$$

$$-\left[\frac{B}{2}(t-4d) + \frac{1}{3}\left(\frac{B}{2}\right)^3 (t-4d)^2(t+8d)\right][U(t) - U(t-4d)] + \frac{2}{3}(2Bd)^3 U(t). \quad (85)$$

This shows us clearly how the image function tends to a simple triangular pulse within the interval $(0, 4d)$ and is small elsewhere.

Values from (84) both with and without the guided mode term were calculated with a PC using simple routines for the modified Bessel functions [9]. Results are given in Figs. 5 and 6. The convergence is seen to correspond to the expression (85) for the dashed function despite the rapid divergence (83) of the F_n functions. Thus, electrically thin slabs can be analyzed extremely easily using the present theory.

Slightly more effort is needed for the evaluation of the general image functions like (34). We calculated values for the image function $f^{TM}(t)$ for $\epsilon = 2$ for two normalized thicknesses of the slab, $4Bd = 1$ and $4Bd = 2$, Figs. 7,8. Here again, in spite of the inherent divergence of the modified Bessel functions, the image function without the guided mode term (dashed lines) was seen to converge for values of t small enough where the Bessel function routines were accurate.

In addition to the delta function terms, there are also step discontinuities at the values $t = 4md$ of the argument. It is not difficult to find exact expressions for these step discontinuities of the image function, in fact, from the $k = 0$ terms of (34) we obtain

$$\frac{2}{B}\Delta f^{TM}(t) = E^{2m-1}(1 - E^2)B4md \quad \text{at} \quad t = 4md. \quad (86)$$

There are obviously no step discontinuities when $\epsilon = 1$ (Figs. 5, 6) or $\epsilon = \infty$. The largest step will occur at $m = (\epsilon + 1)^2/4\epsilon$. The first step is largest for $\epsilon < 5.8$. With the present PC and simple Bessel function routines, the applicability of the expressions seems to end at about $\epsilon \approx 4$ with moderate thicknesses of the slab (only first modes propagating). Thus, the method seems to be best suited at the moment for microstrip antenna structures, where low ϵ is desired.

The function $f^{TE}(t)$ is of the same form as the corresponding $f^{TM}(t)$ function and can be obtained from it after the interchange $\epsilon \leftrightarrow \mu$ and change of sign. Evaluation of the more complicated $f_0(t)$ function and the corresponding transmission image functions must be left to a future work. It is hoped that an easier analytic form for the image functions could be found with the modified Bessel functions replaced by functions with intrinsic convergence properties. Since the exact expressions have been already derived, it seems to be a question of finding suitable analytic transformations for these functions. The residue series method applied in [3] is, of course, one such possibility, leading to a series of exponential functions, but it has the inconvenience of requiring a determination of a set of poles from solutions of a transcendental equation and, thus, does not yield the luxury of an explicit expression.

CONCLUSION

The exact image method has been extended to problems involving a slab with ϵ and/or μ different from those of the surrounding space. Both reflection and transmission image expressions have been derived and their validity studied with asymptotic tests. Numerical convergence has been demonstrated with calculations. With the present experience, using a PC and simple routines for the modified Bessel functions, the method appears to work for values of $\epsilon < 3$ and moderate thicknesses of the slab and, thus, be of interest for the analysis of microstrip antennas. Further effort should be directed to transforming the present exact expressions into other forms for the extension of their numerical range of validity in microcomputer calculations.

ACKNOWLEDGEMENT

This work was carried out while the author was on sabbatical leave as a visiting scientist at the Research Laboratory of Electronics, MIT, during the academic year 1986-87. The author is indebted to professor Jin Au Kong for this possibility and for fruitful discussions upon the present topic. The help from my son, Antti Lindell, in preparing computer codes and graphs is also gratefully acknowledged.

REFERENCES

[1] I.V. Lindell, E. Alanen, "Exact image theory for the Sommerfeld half-space problem. Parts I, II, III," *IEEE Trans. Antennas Propagat.*, vol. AP-32, pp. 126-133, 841-847, 1027-1032, 1984.

[2] I.V. Lindell, E. Alanen, H.von Bagh, "Exact image theory for the calculation of fields transmitted through a planar interface of two media,"*IEEE Trans. Antennas Propagat.*, vol. AP-34, no. 2, pp. 129-137, Feb. 1986.

[3] E. Alanen, I.V. Lindell, A.T. Hujanen, "Exact image method for field calculation in horizontally layered medium above a conducting ground plane," *IEE Proc.*, vol. 133, pt.H, no.4, pp. 297-304, Aug. 1986.

[4] I.V. Lindell, E. Alanen, A.T. Hujanen, "Exact image theory for the analysis of microstrip structures", *Jour. Electromagnetic Waves Appl.*, vol.1, no.2, pp. 95-108, 1987.

[5] J.R. Mosig, "Backside radiation from a microstrip patch antenna", *1986 National Radio Science Meeting*, Philadelphia, p.182, June 1986.

[6] J.A. Kong, *Electromagnetic Wave Theory*, Wiley 1986, p.327.

[7] M. Abramowitz, I.A. Stegun, *Handbook of Mathematical Functions.* New York: Dover, 1968, p. 378.

[8] I.V. Lindell, Elements of dyadic algebra and its application in electromagnetics. *Helsinki Univ. Tech. Radio Lab. Rept* S126, 1981.

[9] W.H. Press *et al.*, *Numerical Recipes.* New York: Cambridge Univ. Press, 1986.

FIGURE CAPTIONS

Figure 1. Schematic representation of the partial waves in the slab problem showing the multiple reflections and transmissions resulting in the total reflection and transmission coefficients for a plane wave (Fourier space component) arising from the original source. The rays, actually parallel to the z axis, are drawn at an angle for clarity.

Figure 2. Graphical method for the construction of roots corresponding to the lowest TE and TM guided modes in the slab of thickness $2d$.

Figure 3. Values of the attenuation factor of a guided wave in the slab, $\alpha_p d$ for different values of the parameters Bd and γ. Both TE (with $\gamma = \mu$) and TM (with $\gamma = \epsilon$) cases are covered by the same diagram.

Figure 4. Normalized function $F_n(c,t)$ for different values of n and Bc.

Figure 5. Normalized image function $f^{TM}(t)$ (solid line), as calculated from (84), and the same with the residue (guided mode) image term extracted (dashed line) in the case $\epsilon = 1$, $\mu \neq 1$, $4Bd = 1$. The corresponding function $f^{TE}(t)$ for $\mu = 1$, $\epsilon \neq 1$, $4Bd = 1$ is obtained by merely changing the sign.

Figure 6. The same as Fig. 5, with $4Bd = 2$.

Figure 7. Normalized image function $f^{TM}(t)$, without the delta function terms, calculated from (34a) (solid line) and the same with the residue (guided mode) term extracted (dashed line) for $\epsilon = 2$, $4Bd = 1$. The corresponding function $f^{TE}(t)$ for $\mu = 2$, $4Bd = 1$ is obtained by merely changing the sign.

Figure 8. The same as Fig. 7, with $4Bd = 2$.

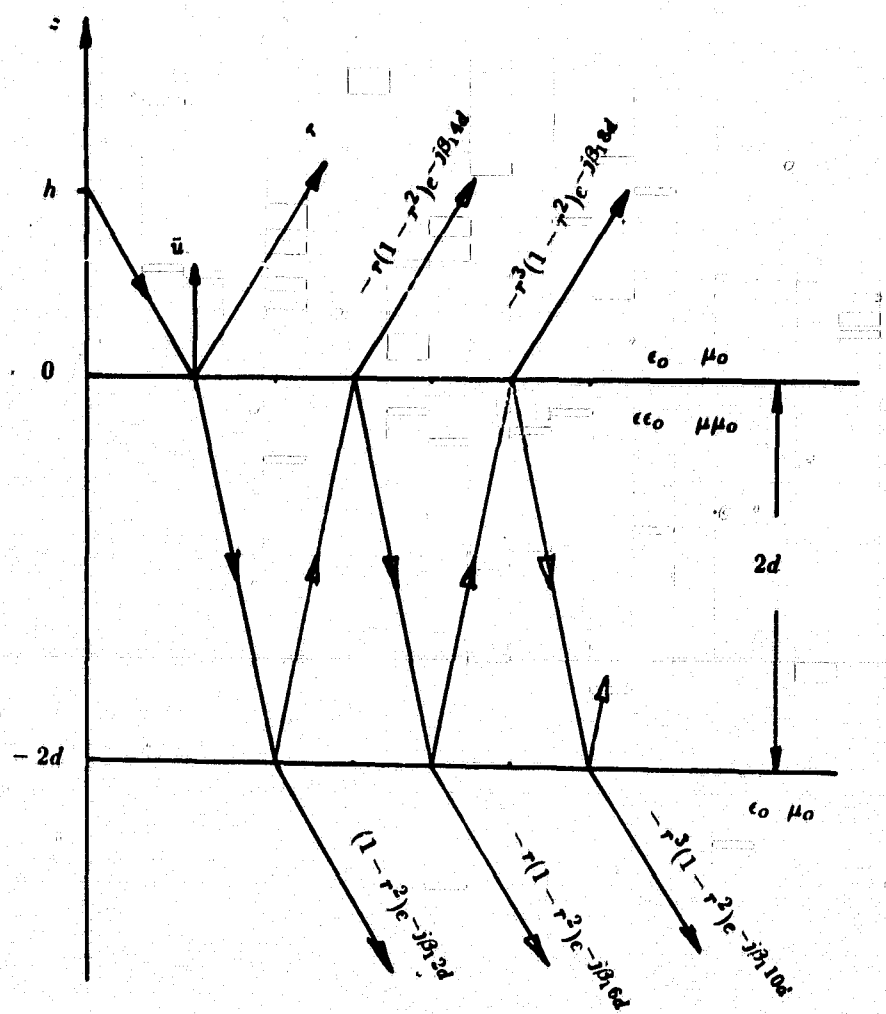
z
h
0
-2d
2d
ū
r
$-r(1-r^2)e^{-j\beta_1 4d}$
$-r^3(1-r^2)e^{-j\beta_1 6d}$
ϵ_o μ_o
$\epsilon\epsilon_o$ $\mu\mu_o$
ϵ_o μ_o
$(1-r^2)e^{-j\beta_1 2d}$
$-r(1-r^2)e^{-j\beta_1 6d}$
$-r^3(1-r^2)e^{-j\beta_1 10d}$

Figure 1

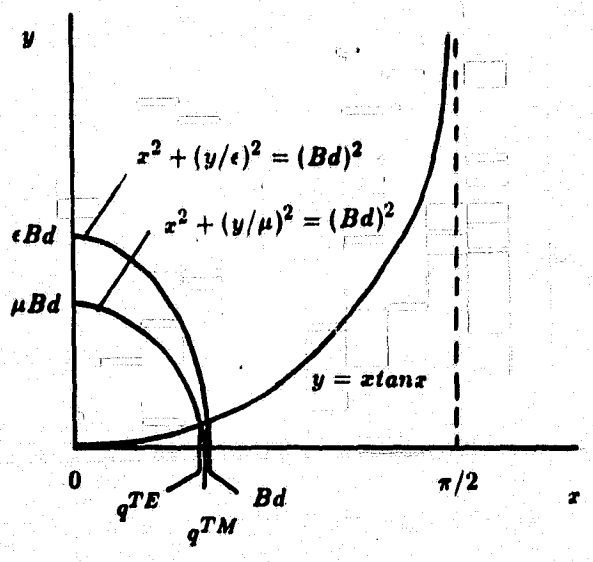
y
$x^2 + (y/\epsilon)^2 = (Bd)^2$
$x^2 + (y/\mu)^2 = (Bd)^2$
ϵBd
μBd
$y = x\tan x$
0
q^{TE}
q^{TM}
Bd
$\pi/2$
x

Figure 2

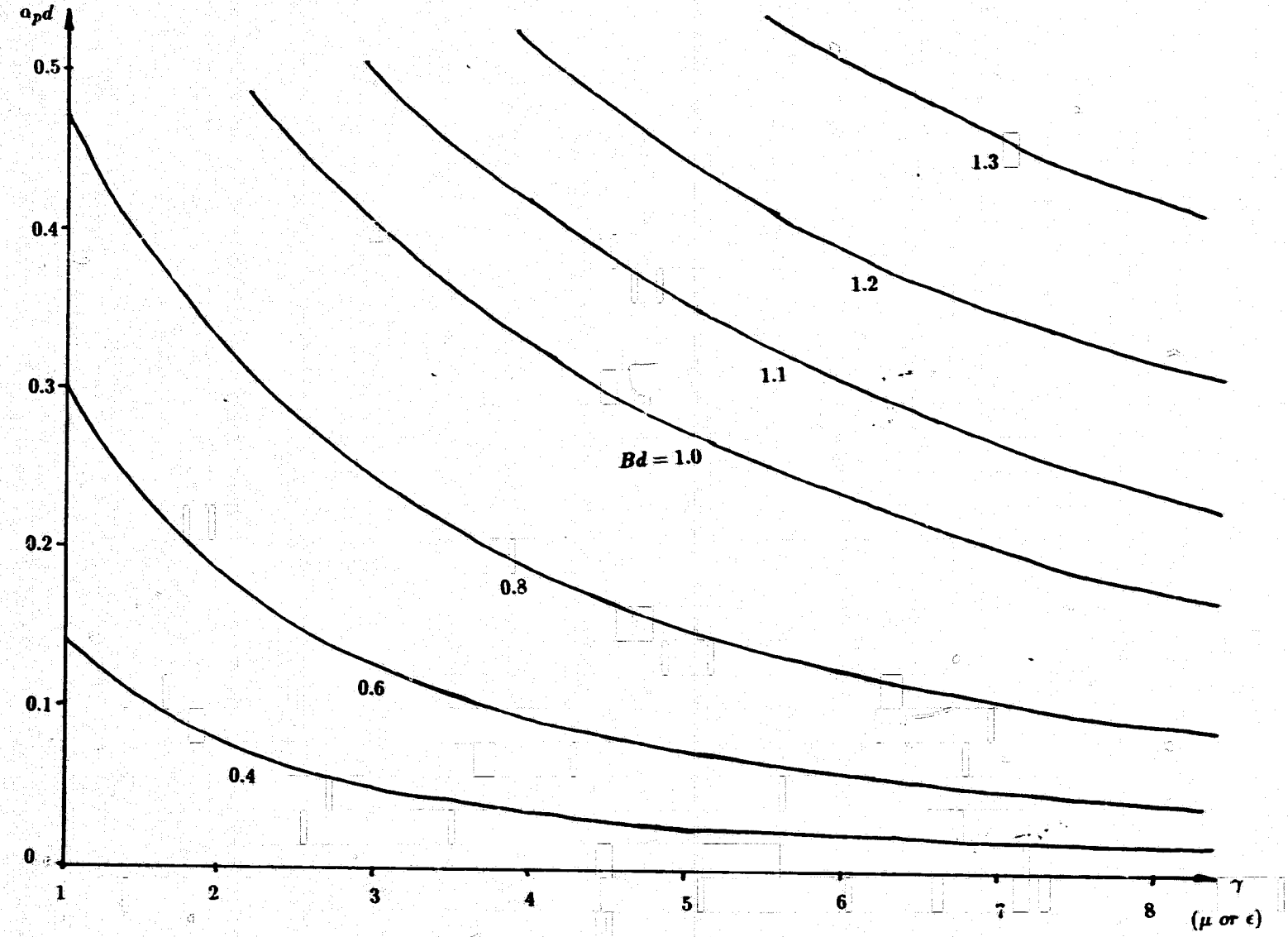
a_{pd}
0.5
0.4
0.3
0.2
0.1
0
1
2
3
4
5
6
7
8
γ
(μ or ϵ)
1.3
1.2
1.1
$Bd = 1.0$
0.8
0.6
0.4

Figure 3

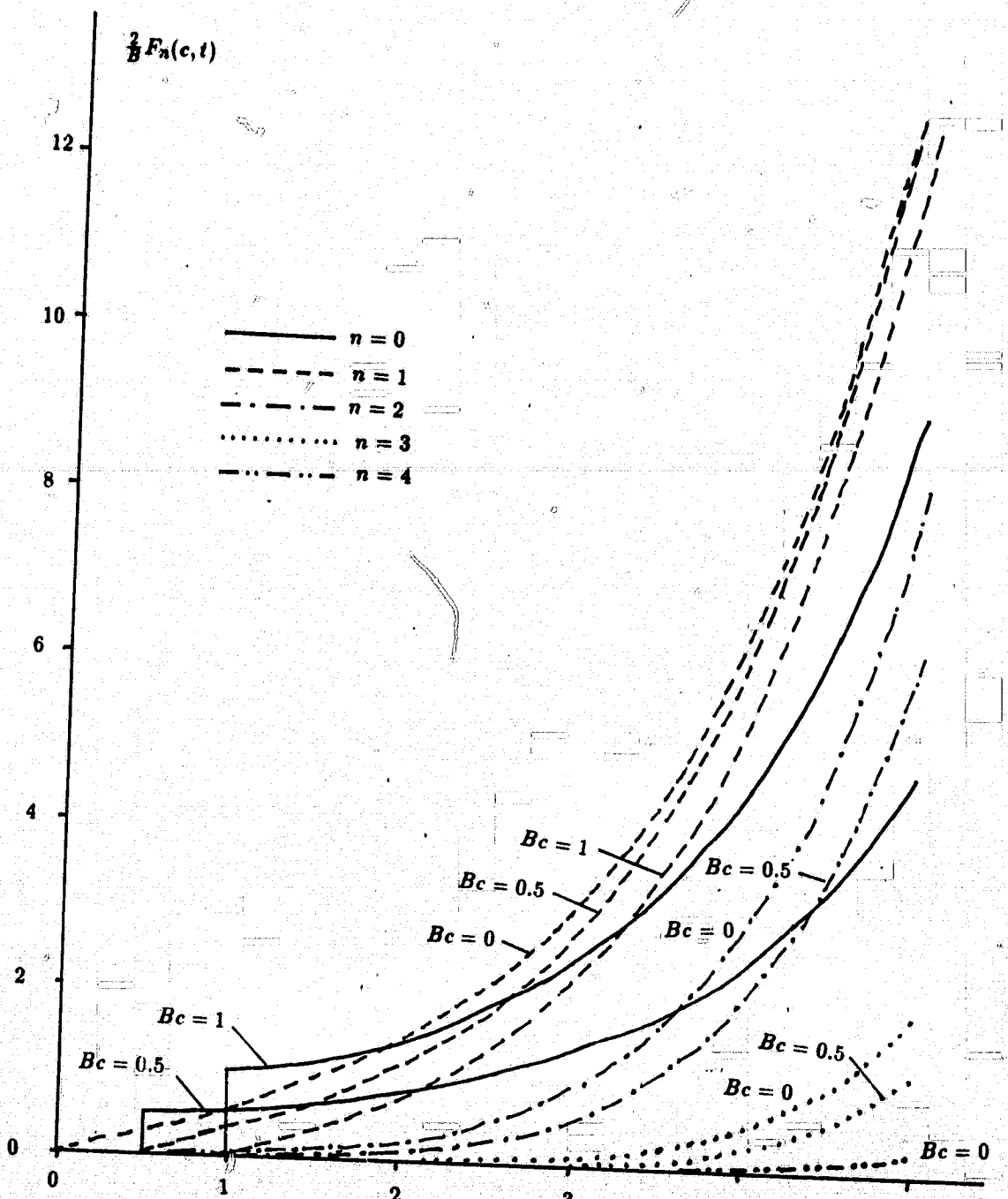
$\frac{2}{B}F_n(c,t)$
12
10
8
6
4
2
0
0
1
2
3
4
5
Bt
n = 0
n = 1
n = 2
n = 3
n = 4
Bc = 1
Bc = 0.5
Bc = 0
Bc = 1
Bc = 0.5
Bc = 0
Bc = 0.5
Bc = 0
Bc = 0

Figure 4

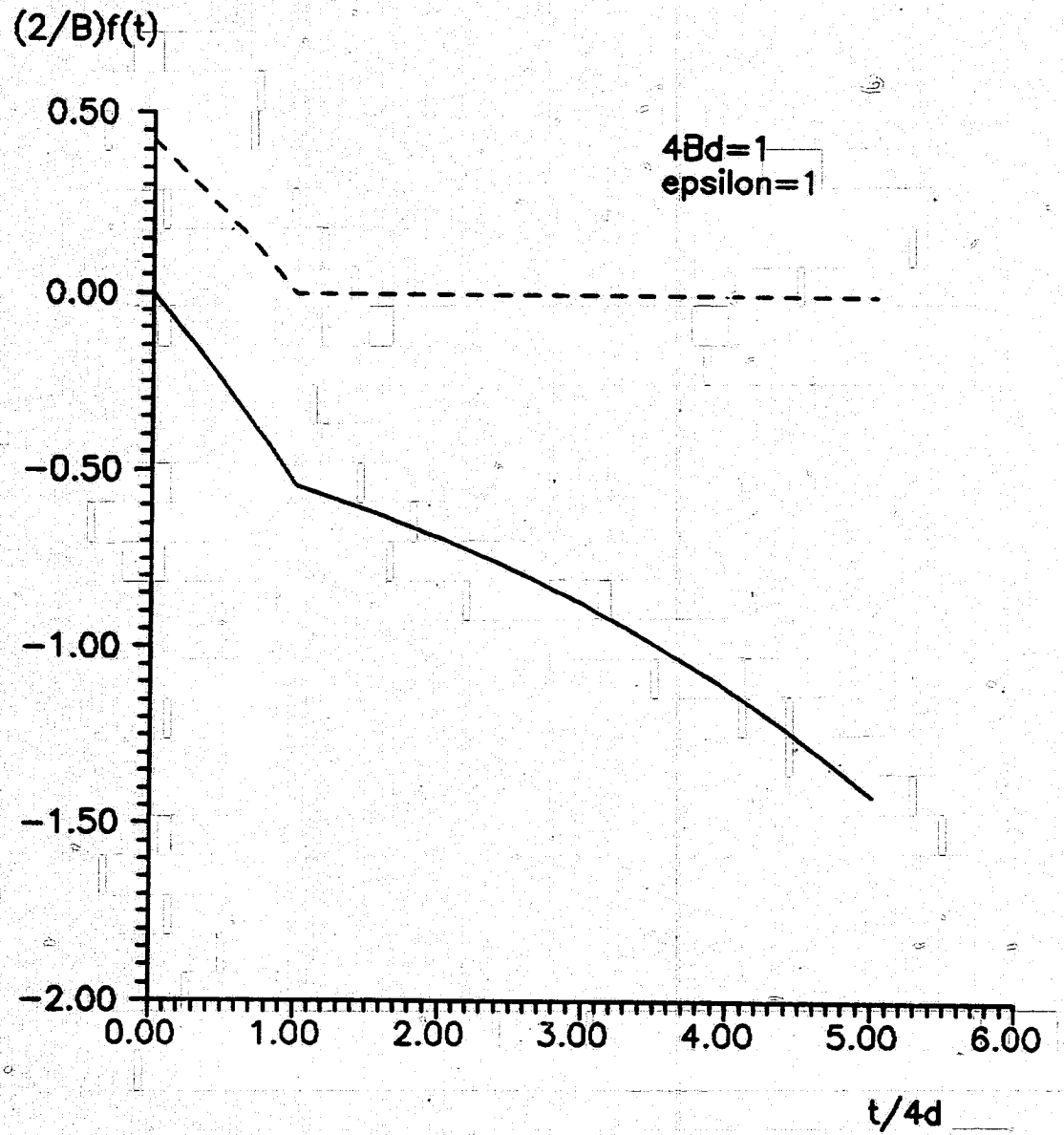
(2/B)f(t)
0.50
0.00
−0.50
−1.00
−1.50
−2.00
0.00
1.00
2.00
3.00
4.00
5.00
6.00
t/4d
4Bd=1
epsilon=1

Figure 5

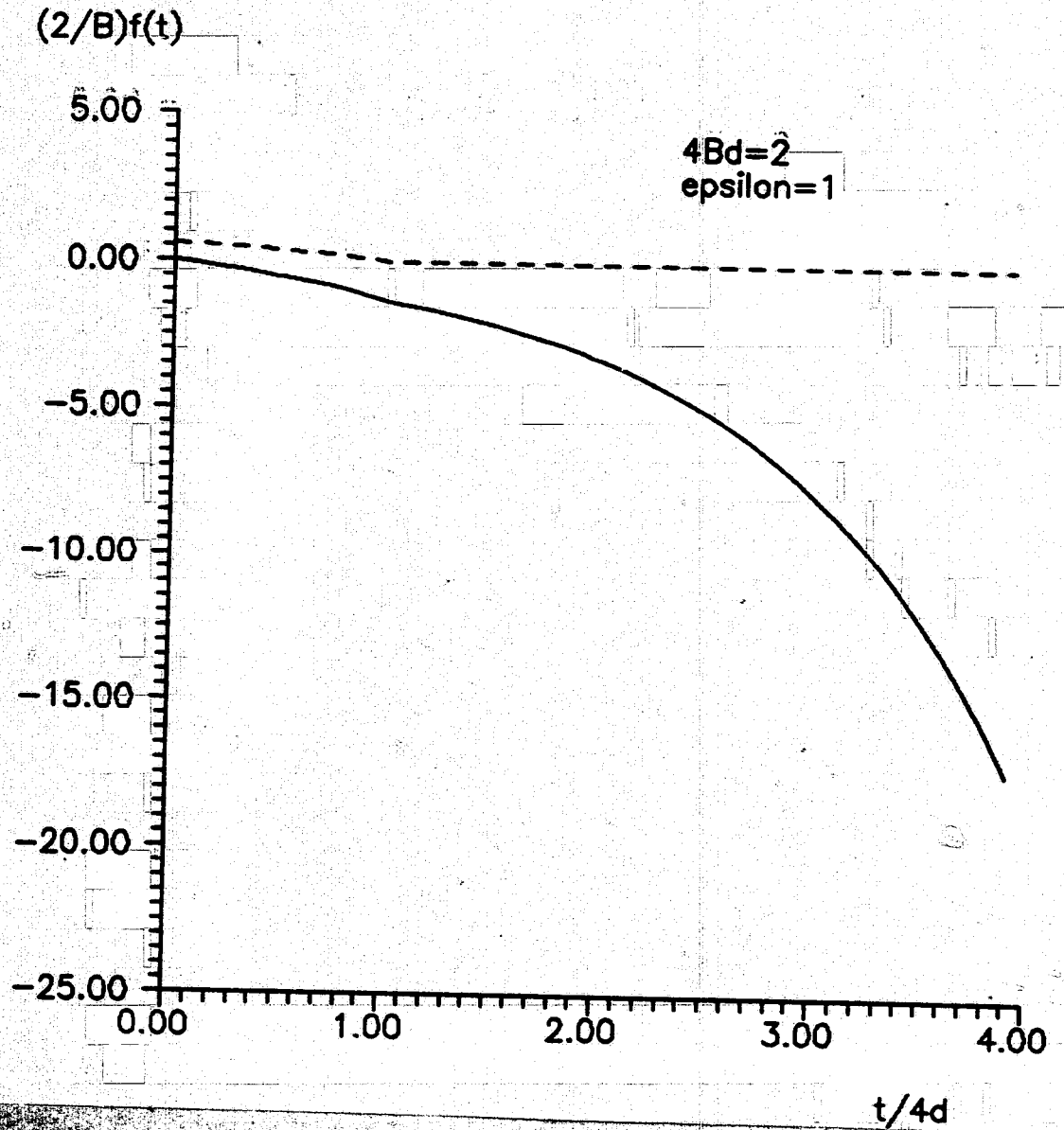
(2/B)f(t)
5.00
0.00
-5.00
-10.00
-15.00
-20.00
-25.00
4Bd=2
epsilon=1
0.00
1.00
2.00
3.00
4.00
t/4d

Figure 6

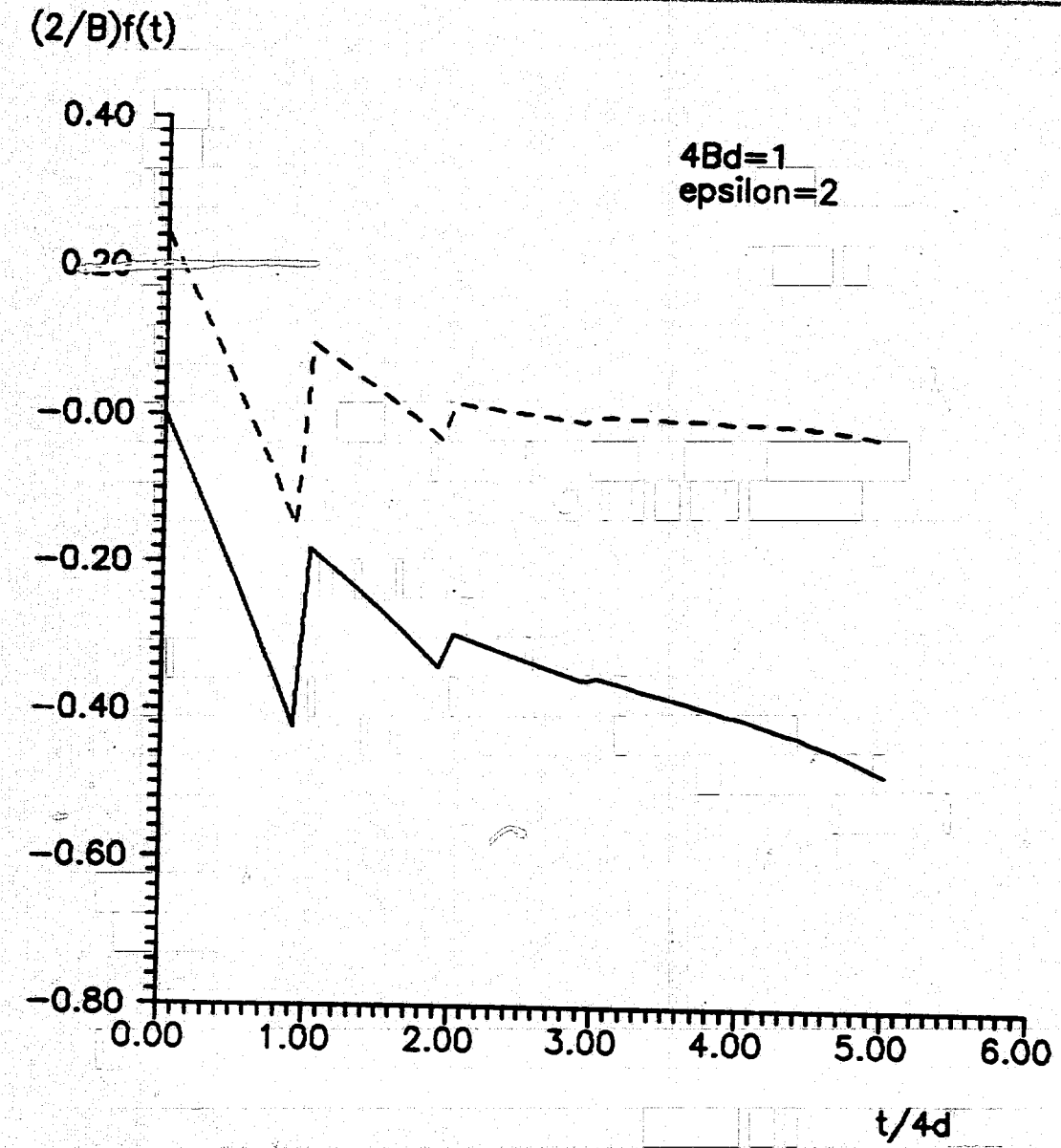
(2/B)f(t)
4Bd=1
epsilon=2
0.40
0.20
-0.00
-0.20
-0.40
-0.60
-0.80
0.00
1.00
2.00
3.00
4.00
5.00
6.00
t/4d

Figure 7

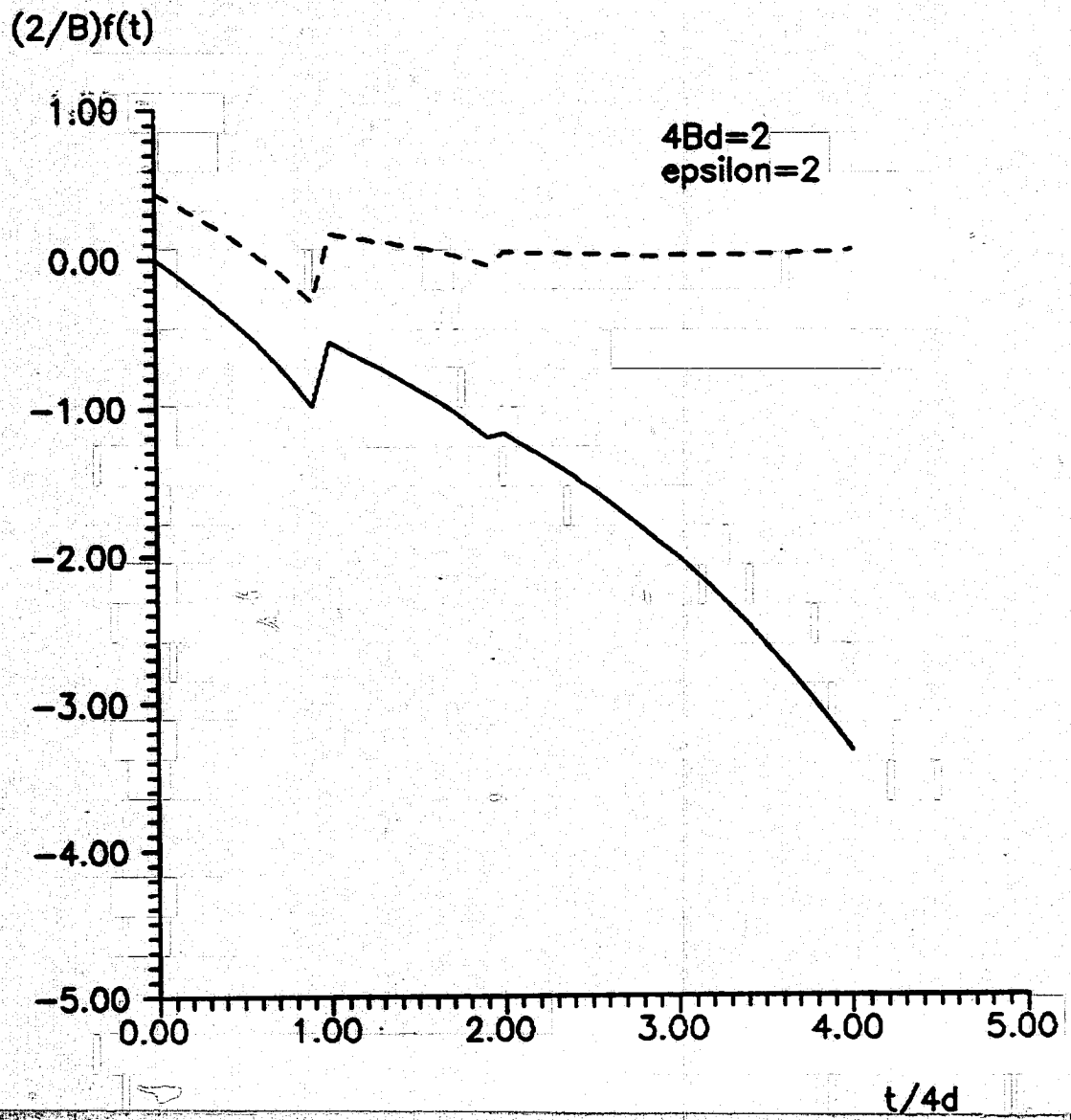
(2/B)f(t)
1.00
0.00
-1.00
-2.00
-3.00
-4.00
-5.00
0.00
1.00
2.00
3.00
4.00
5.00
t/4d
4Bd=2
epsilon=2

Figure 8